



Laser cladding AA2014 with a Al-Cu-Si compound for increased wear resistance

by K.J. Kruger* and M. du Toit*

Paper written on project work carried out in partial fulfilment of B. Eng. (Metallurgical Engineering)

Synopsis

Aluminium alloys have gained popularity in many industries due to their high strength and low weight. One shortcoming of aluminium alloys is their poor resistance to abrasion and erosion wear compared to materials such as stainless steels. In this project, aluminium alloy 2014 (AA2014) was coated with a 1.5 mm thick laser-deposited layer composed of silicon, copper, and aluminium with the aim of increasing the wear resistance. The amount of silicon, copper, and aluminium added to each sample was determined by a mixtures model. It was discovered that the Al-Cu system is very sensitive to silicon additions and that wear resistance depends on the primary phase to solidify as well as on the final phase distribution. Two primary phases were identified; alpha aluminium and theta intermetallic. It was observed that the clad layer increases both the hardness and wear resistance of AA2014, and that the material solidifying as primary alpha aluminium displayed a lower hardness but higher wear resistance than the samples containing primary theta phase. All clad layers performed better in terms of wear resistance than the unclad samples. The knowledge gained and principles used in this project could be applied to many other aluminium alloys.

Keywords

aluminium alloys, laser cladding, wear resistance.

Introduction

AA2014 is a lightweight and high-strength material that has proven invaluable in applications that require a high strength-to-weight ratio. The alloy finds most of its applications in the aerospace industry, although new inroads into the drill piping industry have been established. Due to the low alloying element content in AA2014, the material displays poor hardness and, therefore, poor wear resistance. There is therefore a need to increase the wear resistance of AA2014 without altering the bulk mechanical properties such as ductility and strength-to-weight ratio.

Scientific background

Due to the low alloying element content, AA2014 is not particularly hard and is therefore not abrasion resistant. This is the case for most 2000 series aluminium alloys,

and it has become desirable for industrial application to increase the wear resistance of these alloys without compromising the material's strength or strength-to-weight ratio. The alloy composition and relevant mechanical properties are shown in Tables I and II respectively.

A potential solution to the low wear resistance of AA2014 is to coat the material with a wear-resistant layer. This project will consider the use of laser cladding an Al-Cu-Si compound onto the AA2014 substrate with the intention of increasing the wear resistance of the surface while leaving the bulk mechanical properties of the material unchanged. The aim of this cladding process is to produce a harder material by intermetallic phase formation between aluminium and copper in the form of Al_2Cu . This intermetallic phase formation as well as the microstructure can be seen in Figure 1. This microstructure was achieved using a 40 wt% Cu 60 wt% Al clad composition (Dubourg, 2002). It was found that the intermetallic phase was the first to solidify, and the resulting hardness and abrasion resistance was the highest in the alloy range that was tested.

In the current investigation, silicon was added in an attempt to minimize porosity in the cladding. If successful, this cladding process could be applied to many aluminium alloys in which wear resistance is important but impractical to achieve by conventional methods. Tough alloys that do not necessarily display good wear characteristics could be surfaced using this process to increase the resistance to abrasive wear while maintaining the toughness of the bulk material.

* Department of Materials Science and Metallurgical Engineering, University of Pretoria, Pretoria, South Africa.

© The Southern African Institute of Mining and Metallurgy, 2014. ISSN 2225-6253. Paper received Jan. 2014.

Laser cladding AA2014 with an Al-Cu-Si compound for increased wear resistance

Table I

Typical chemical composition (in weight %) of aluminium alloy AA2014. Single values denote maximum limits. (Capalex, 2013)

| %Cu | %Fe | %Si | %Mn | %Mg | %Cr | %Zn | %Ti | %Other | %Al |
|---------|-----|-----|---------|---------|-----|------|------|--------|---------|
| 3.8–4.9 | 0.5 | 0.5 | 0.3–0.9 | 1.2–1.8 | 0.1 | 0.25 | 0.15 | 0.15 | Balance |

Table II

Typical mechanical properties of AA2014 in the T4, T351 heat-treated condition (Kaufman, 2002)

| Ultimate tensile strength (MPa) | Yield strength (MPa) | Brinell hardness number (500 kg/ 10 mm) | Modulus of elasticity (GPa) |
|---------------------------------|----------------------|---|-----------------------------|
| 472 | 325 | 120 | 73 |

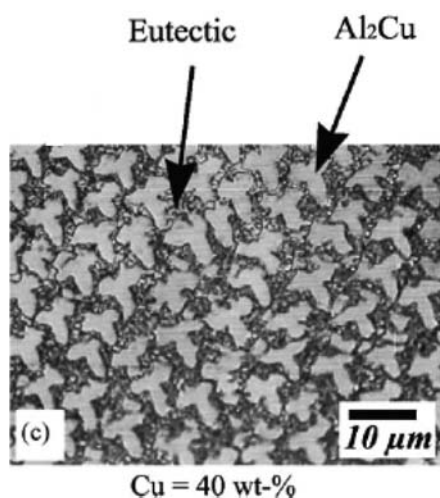


Figure 1—Microstructure of laser-clad 40%Cu-Al material forming primary intermetallics and a secondary eutectic phase etched with Keller's reagent (Dubourg, 2002)

Literature review

Laser cladding

Laser cladding is a low heat input, rapid solidification process. The advantages of this process include high levels of productivity due to fast welding speeds, low levels of dilution, refined microstructures due to rapid solidification, minimal distortion of the work piece, and small heat-affected zones (HAZs) (CSIR, 2012). There is a general consensus on the advantages of laser cladding in these respects, regardless of the cladding feed material or substrate being clad (Liu, 1995; Hyatt, 1998; CSIR, 2012; Joining Technologies, 2012). This process makes it possible to bond a material with a completely different microstructure and mechanical properties to a substrate. The process makes use of high-intensity light emission that is focused using several lenses to a point above, below, or on the surface of the work piece depending on the intended application (Joining Technologies, 2012). In

the case of laser cladding, the focal point of the beam is slightly above the work piece so as to melt the feed material without melting much of the substrate. This causes minimal dilution and rapid solidification of the feed material onto the substrate while ensuring that a metallurgical bond is achieved. These properties are desirable for the above-mentioned application. This will result in little to no change in the substrate bulk properties while achieving the desired result of depositing a layer of feed material that will act as an abrasive-resistant coating.

A powder feeder was used to feed the material into the weld pool via a carrier gas. The powder feeder method was chosen over other methods, such as preplaced powders, because it is the only method that is industrially viable (Vilar, 2001). Figure 2 illustrates the process of laser cladding using a powder feed. It can be observed from the schematic that the powder is fed into the weld pool via a powder injection nozzle and is transported in space by a carrier gas. Once the powder enters the weld pool, it melts and will rapidly solidify to form a coating as the laser moves along the track.

Cladding material

An important microstructural aspect to consider when selecting materials suitable for wear resistance is the presence of a finely distributed hard phase in a matrix of a more ductile phase. It is also important to ensure that the

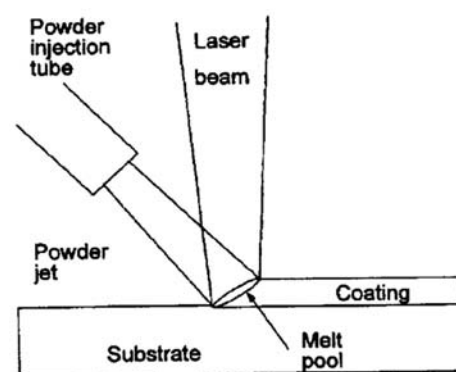


Figure 2—Schematic of laser cladding using a powder feeder (Vilar, 2001)

Laser cladding AA2014 with an Al-Cu-Si compound for increased wear resistance

cladding material is compatible with the substrate and that no brittle phases are formed along the fusion line that could result in poor metallurgical bonding.

When considering an abrasion-resistant layer, the most important aspect is the cladding hardness. There is a general consensus in the literature that material hardness is directly proportional to abrasion resistance (Kim, 2006; Jeong, 2003; Caldwell, 1988). This is due to the fact that harder materials are more resistant to plastic deformation and will therefore resist the process of wear more effectively than softer material. Figure 3 illustrates the effect of hardness on the wear resistance of pure metals and several steel alloys.

From Figure 3 it is clear that, in general, as the hardness of a material increases, so does its abrasion wear resistance.

It can be observed from the results of the study by Dubourg (2002) that the wear resistance of the layer is directly related to cladding hardness. Figure 4 is a graphical representation of the wear resistance of an aluminium sample as the copper content is increased.

Figure 5 shows a graphical representation of the hardness of the clad material measured at varying depths prior to any post-cladding heat treatment (Dubourg, 2002). It is evident that an increase in copper content increases the hardness of the clad layer. The material displays a rapid drop in hardness at a depth of approximately 0.9 mm, most likely due to the transition into the virgin aluminium base material.

Figure 5 indicates that the hardness of the cladding increases with copper content. This is due to an increase in the amount and particle size of the intermetallic θ phase.

Figure 6 displays the equilibrium Al-Cu binary phase diagram. It can be seen that the eutectic composition is at 33 wt% Cu; however, this true only for the binary system under equilibrium conditions.

Pseudo-binary Al-Cu-Si phase diagrams are considered in Figures 7 and 8 at 1% and 10% silicon respectively. It is clear that as the silicon concentration of a sample is increased, the

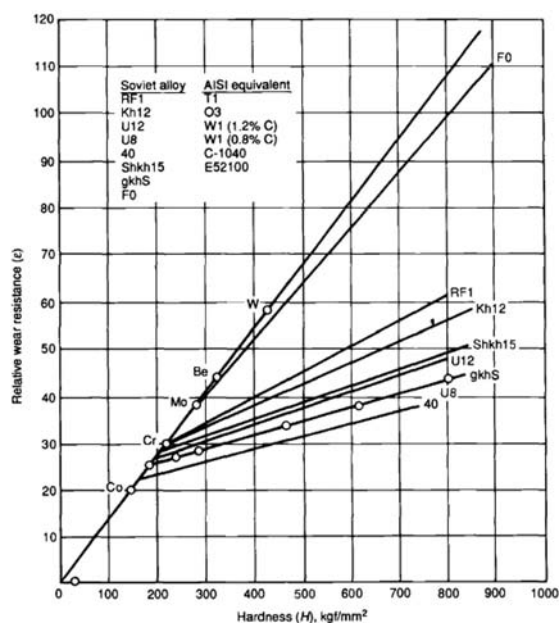


Figure 3—The relationship between wear resistance and hardness in several pure metals and alloys (Tylczak, 1992)

formation of primary theta phase is favoured at lower concentrations of copper. The formation of either primary alpha aluminium or primary theta phase could affect the mechanical properties of the material and must therefore be carefully monitored.

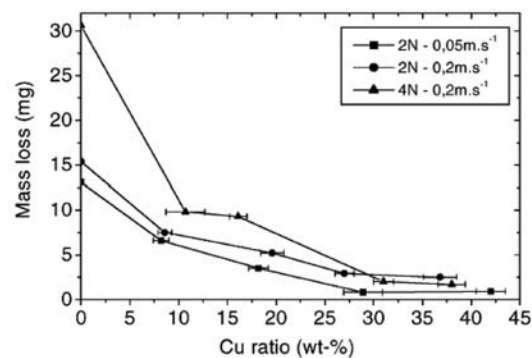


Figure 4—Graphical representation of the decrease in wear rate under different wear parameters with increasing copper content in the cladding material (Dubourg, 2002)

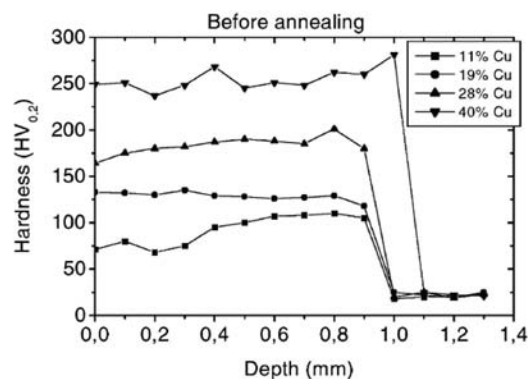


Figure 5—Graphical representation of hardness for various cladding compositions as a function of depth (Dubourg, 2002)

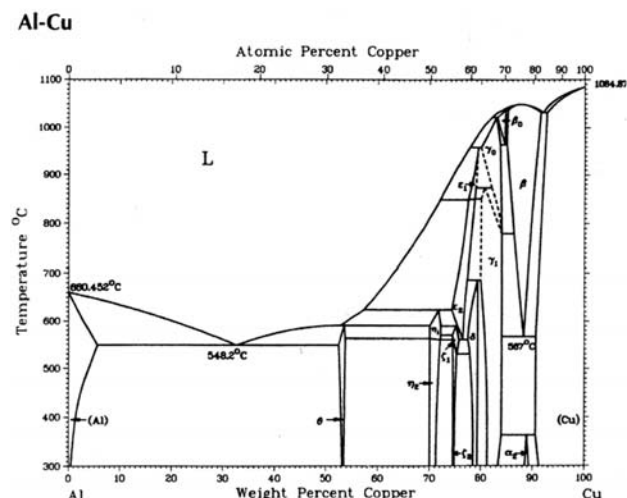


Figure 6—Aluminium-copper phase diagram (Murray, 1992)

Laser cladding AA2014 with an Al-Cu-Si compound for increased wear resistance

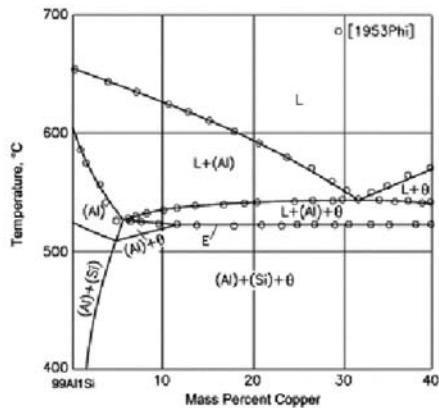


Figure 7—Vertical section of the Al-Cu-Si phase diagram containing 1% Si (Raghavan, 2007)

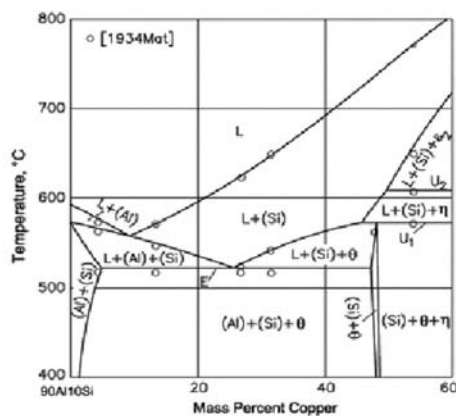


Figure 8—Vertical section of the Al-Cu-Si phase diagram containing 10% Si (Raghavan, 2007)

Methodology

Twelve samples were laser-clad with layers containing from 30–54 wt% copper and 0–3.4 wt% silicon (Table III). One sample remained unclad and was subjected to the same testing procedure as a control:

The layer compositions were selected using a statistical method known as the mixture lattice design. This design was chosen to maximize the useful data that is extractable from the experiments and allow for the mapping of material characteristics based on chemistries using contour lines..

The centre point in the experiment (samples 1, 6, and 12) was performed in triplicate in order to test the consistency of the cladding process.

The samples were produced by gas-feeding three powders (pure Cu, pure Al, and 12%Si-Al alloy) from three hoppers into the weld pool via a triaxial nozzle.

The laser parameters used to produce the samples are listed in Table IV.

These parameters produced a smooth, well-bonded clad layer, but have not been optimized for all the samples. After polishing, some unmelted particles were observed in the inter-bead region of most samples.

The clad samples were subjected to chemical analysis, micro-Vickers hardness tests, and microstructural analysis

using optical emission spectrometry (OES), as optical microscopy, and scanning electron microscopy using energy-dispersive spectroscopy (SEM-EDS). Based on the results of these tests, two samples were selected for wear testing, together with the unclad control sample.

Results and discussion

The results from the OES chemical analysis, micro-Vickers hardness tests, and SEM-EDS phase analysis are displayed in Table V.

Chemical analysis

It is evident from the Table V that while the silicon content was acceptable in each case, the copper content in all samples was consistently lower than the designed copper content. This implies a problem with the copper delivery system. A possible solution would be pre-mixing of the powders and using only one hopper.

The system is very sensitive to silicon content and for this reason, unexpected solidification patterns were observed. Several samples solidified as primary α -Al while others solidified as primary θ -intermetallic.

Localized EDS measurements indicated that neither the primary nor the eutectic phase contained silicon values higher than 1%. Microstructural examination of the cladding was therefore carried out.

Microstructure

The addition of silicon promotes the formation of primary θ

Table III

Example of a table used to capture experimental data (weight %) (Balance is aluminium)

| Sample no. | Si content in clad (%) | Cu content in clad (%) |
|------------|------------------------|------------------------|
| 1 | 0 | Unclad control |
| 2 | 0 | 30 |
| 3 | 1.1 | 37.1 |
| 4 | 2.3 | 44.3 |
| 5 | 3.4 | 51.5 |
| 6 | 0 | 42 |
| 7 | 2.3 | 44.3 |
| 8 | 4.5 | 46.5 |
| 9 | 6.8 | 48.8 |
| 10 | 0 | 54 |
| 11 | 1.1 | 49.2 |
| 12 | 2.3 | 44.3 |
| 13 | 3.4 | 39.5 |

Table IV

Final laser parameters

| Laser parameter | Final value |
|--------------------------------------|-------------|
| Power | 2.5 kW |
| Spot size | 3 mm |
| Step-over distance | 0.8 mm |
| Resultant overlap | 73.3% |
| Welding speed | 1.5 m/min |
| Gas flow rate (1.5 l/min per hopper) | 4.5 l/min |

Laser cladding AA2014 with an Al-Cu-Si compound for increased wear resistance

Table V
Results of chemical analysis, hardness tests, and phase analysis

| Sample no. | Design Si content in clad (wt %) | Design Cu content in clad (wt %) | Hardness (HV) | OES analysed Si content (wt %) | OES analysed Cu content (wt %) | Phases present |
|------------|----------------------------------|----------------------------------|---------------|--------------------------------|--------------------------------|------------------|
| 1 | 2.3 | 44.3 | 243 | 2.2 | 33.3 | Al+ θ |
| 2 | 1.1 | 37.1 | 234 | 1.1 | 28.5 | Al+ θ |
| 3 | 0 | 30 | 214 | 0.2 | 22.3 | Al+ θ |
| 4 | 3.4 | 51.5 | 370 | 3.1 | 39.7 | Al+ θ +Si |
| 5 | 0 | 42 | 277 | 0.2 | 31.6 | Al+ θ |
| 6 | 2.3 | 44.3 | 225 | 2.1 | 31.8 | Al+ θ |
| 7 | 4.5 | 46.5 | 259 | 4.2 | 35.4 | Al+ θ +Si |
| 8 | 6.8 | 48.8 | 250 | 6 | 33.5 | Al+ θ +Si |
| 9 | 0 | 54 | 260 | 0.2 | 41.5 | Al+ θ |
| 10 | 1.1 | 49.2 | 265 | 1.2 | 39.2 | Al+ θ |
| 11 | 3.4 | 39.5 | 203 | 3.2 | 32 | Al+ θ +Si |
| 12 | 2.3 | 44.3 | 199 | 2.1 | 33 | Al+ θ |
| 13 | Control | Control | 116 | | | |

phase, which was apparent in the microstructure of most samples (as seen in Figure 9). However, the primary α phase formed in several samples, (Figure 10).

It can be seen from Figure 9 that there is a large amount of primary θ phase and very small amounts of eutectic phase in the microstructure of sample 9. This is considered to be the desired microstructure due to the large amounts of hard intermetallic phase surrounded by a more ductile eutectic phase.

As shown in Figure 10, sample 12 displays primary phase solidification and this results in soft particles that are surrounded by the harder (α -Al + θ) eutectic phase.

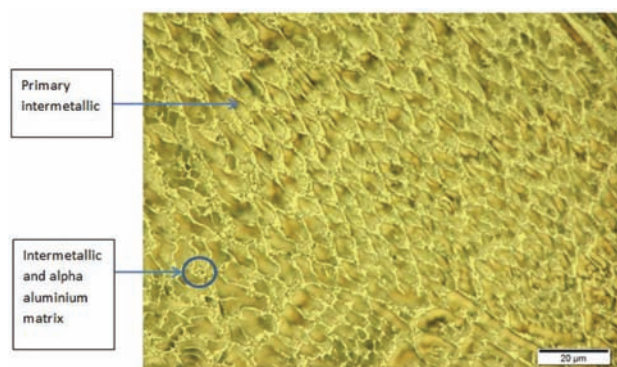


Figure 9—Sample 9, displaying primary theta solidification

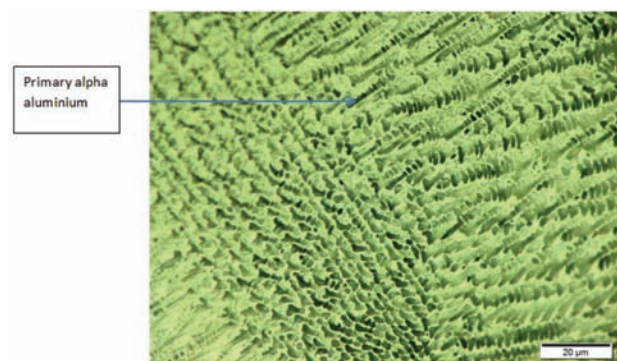


Figure 10—Sample 12 displaying primary alpha solidification

Samples containing higher amounts of silicon (3% and more) contained a third phase, consisting of small grey particles that were visible under an optical microscope. An example of these particles can be seen in Figure 11.

These small grey particles were difficult to identify using SEM back-scatter electron imaging (BEI), and a chemical map was constructed in order to identify the locations of the particles. The results can be seen in Figure 12.

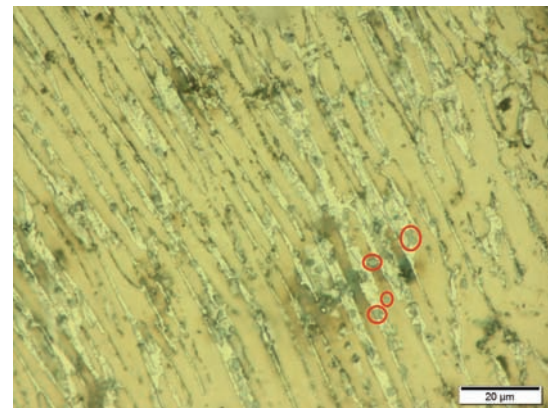


Figure 11—Sample 4, containing tertiary grey phase

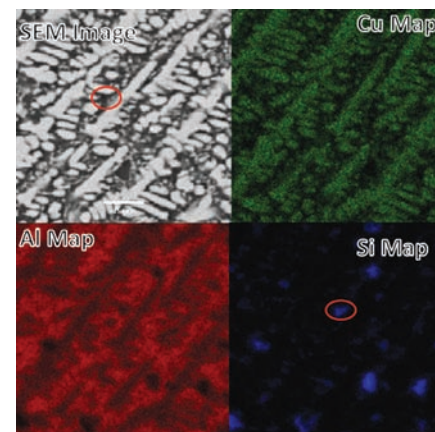


Figure 12—Chemical map of sample 8

Laser cladding AA2014 with an Al-Cu-Si compound for increased wear resistance

It is clear that there are areas of high silicon concentration in this sample and these areas cannot be distinguished from the rest of the microstructure by SEM. The particles could not be accurately analysed using EDS due to their small size, and thermodynamic modelling using FactSage™ was used to predict the equilibrium phases that form on solidification in the samples. The third phase that forms in the high-silicon samples was identified as high-purity (>99%) silicon particles.

When the fusion line was inspected, it was evident that very good metallurgical bonding between the clad layer and the metal substrate had been achieved. This is evident in Figure 13.

The formation of grain boundary precipitates can also be observed; however, these precipitates could be eliminated through solution annealing.

Mechanical properties

Hardness is believed to have the largest influence on the wear resistance of the material, and thus all the samples were subjected to fifteen hardness measurements using the micro-Vickers hardness test. The results were collated and used to generate a hardness contour map with relation to individual sample chemistries, using 'Design Expert' (Figure 14).

It can be seen that high hardness is due to a synergistic effect between copper and silicon.

Wear testing

Based on the results obtained from the above tests, samples 12 and 4 as well as the unclad control sample were subjected to wear testing. Sample 12, which solidified as primary α -Al, displayed the lowest hardness, and sample 4, which solidified as primary θ -intermetallic, displayed the highest hardness. A slurry erosion wear test proved to be too uncontrollable to provide consistent results, and therefore a non-standard, wet two-body abrasion wear test was performed. Tables VI and VII describe the test conditions and results.

It is important to note that the wear test was extremely aggressive and high mass loss was observed. Sample 12 displayed the highest wear resistance, while the unclad sample displayed the lowest wear resistance. Although

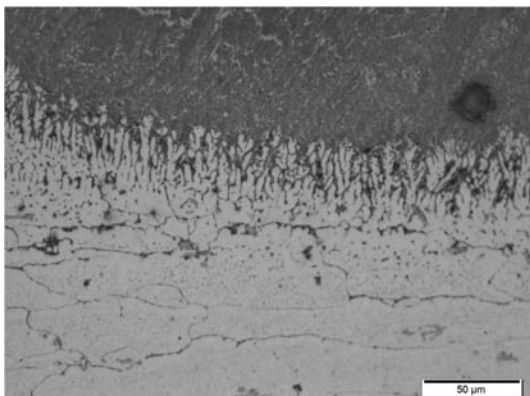


Figure 13—Fusion line between cladding layer (top) and substrate (bottom)

sample 4 had a higher hardness than sample 12, it had a higher mass loss during the wear test. This can probably be attributed to spalling at the sample edges (as shown in Figure 15).

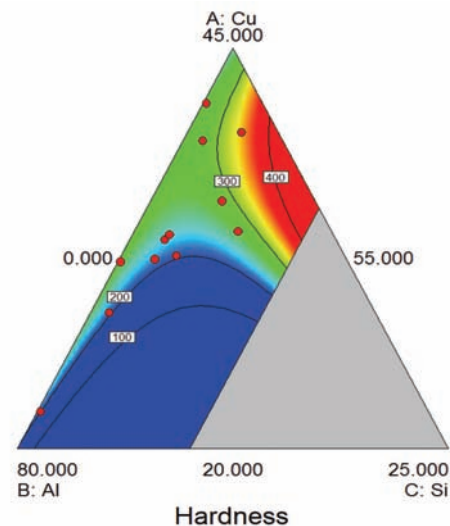


Figure 14—Hardness (HV) contour map based on chemistries obtained from OES results

Table VI

Test conditions in non-standard wet two-body abrasion wear test

| Parameter | Value |
|-------------------------|--------------------------------------|
| Abrasive medium | Diamond-impregnated resin (220 grit) |
| Force applied to sample | 100 N |
| Run time | 10 min |
| Rotation speed | 310 r/min |

Table VII

Mass loss in two-body abrasion wear test

| Sample no. | Mass loss per unit area exposed (g/cm ²) |
|-------------------------|--|
| Control sample (unclad) | 0.162 |
| Sample 4 (hardest) | 0.156 |
| Sample 12 (softest) | 0.134 |

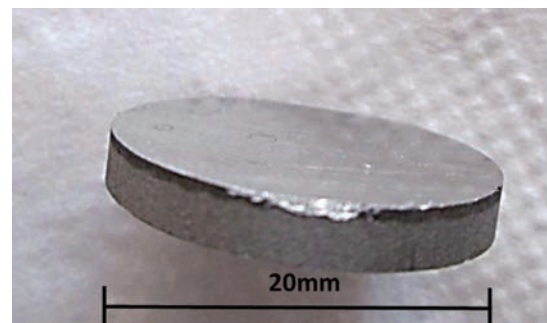


Figure 15—Spalling of sample 4

Laser cladding AA2014 with an Al-Cu-Si compound for increased wear resistance

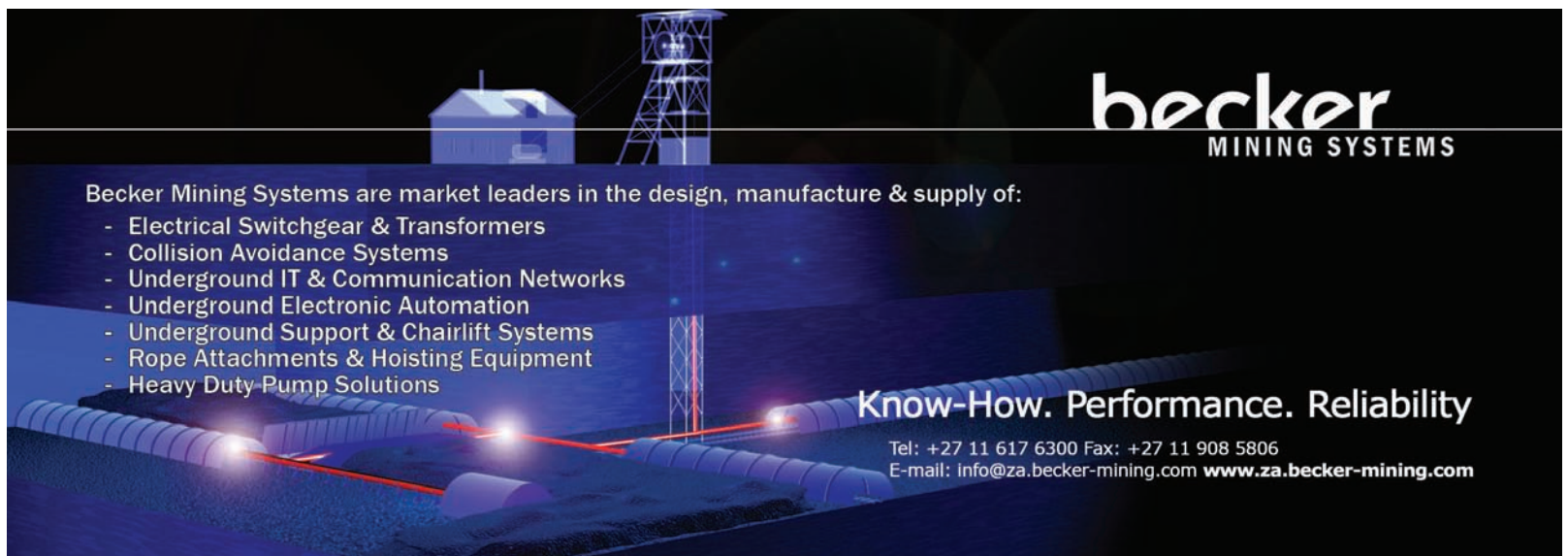
Conclusions

The surface hardness of AA2014 was successfully increased by laser cladding. The effects of the cladding operation were examined using a variety of tests, and an understanding of the mechanisms by which the cladding layer will protect the base material from an abrasive environment has been gained.

This cladding process was successful in providing additional wear resistance as well as hardness to the substrate material without reducing the strength-to-weight ratio of the material. The wear resistance of the material showed a strong correlation to the primary phase that solidifies, and the solidification mechanism is linked to both the thermodynamics and kinetics. It was determined that primary alpha aluminium solidifying samples are more wear-resistant, but have lower hardness than the primary theta phase intermetallic solidifying samples. The reason for the low wear resistance of the hard primary theta solidifying samples is most likely due to spalling. Furthermore, it was determined that both the primary intermetallic and primary alpha aluminium samples were harder and more wear-resistant than the substrate. This implies that the process could be applied to a wide range of aluminium alloys and will broaden the range of application of aluminium alloys by increasing the lifespan of these materials under severe wear conditions.

References

- CALDWELL, S.G. 1988. A microscopic study of the behavior of selected Al-Cu alloys in unlubricated sliding wear*. *Wear*. pp. 225-249.
- CAPALEX. 2013. 2014 alloy data sheet. http://www.capalex.co.uk/alloy_types/2014_alloy.html [Accessed 15 May 2013].
- CSIR. 2012. Laser welding. http://www.csir.co.za/lasers/laser_welding.html [Accessed 13 May 2013].
- DUBOURG, L., PELLETIER, H., VAISSIERE, D., HLAWKA, F., and CORNET, A. 2002. Mechanical characterisation of laser surface alloyed aluminium-copper systems. *Wear*, vol. 253, no. 9. pp. 1077-1085.
- HVATT, C.V. 1998. The Effect of Heat Input on the Microstructure and Properties of Nickel Aluminum Bronze Laser Clad with a Consumable of Composition Cu-9.0Al-4.6Ni-3.9Fe-1.2Mn. *A Metallurgical and Materials Transactions*.
- JEONG, D.H. 2003. The relationship between hardness and abrasive wear resistance of electrodeposited nanocrystalline Ni-P coatings. *Scripta Materialia*. pp. 1067-1072.
- JOINING TECHNOLOGIES. 2012. Laser beam welding. <http://www.joiningtech.com/industry-references/welding-types/laser-beam-welding> [Accessed 9 May 2013].
- KAUFMAN, J.G. 2002. Aluminum alloys. *Handbook of Materials Selection*. Kutz, M. (ed.). John Wiley & Sons. Ch. 4. p. 104.
- KIM, K.T. 2006.
- KYUNG TAE KIM, S. I. 2006. Hardness and wear resistance of carbon nanotube reinforced Cu matrix nanocomposites. *Materials Science and Engineering*. pp. 46-50.
- LIU, Y. 1995. Microstructural Study of the Interface in Laser-Clad Ni-Al Bronze on Al Alloy AA333 and Its Relation to Cracking. *A Metallurgical and Materials Transactions*.
- MURRAY, J. 1992. Binary alloy phase diagrams. *Introduction to Alloy Phase Diagrams*. Vol. 3. Baker, H. (ed.). ASM Handbook, ASM International, Materials Park, OH. p. 2.44.
- RAGHAVAN, V. 2007. Al-Cu-Si. *Journal of Phase Equilibria and Diffusion*. pp. 180-181.
- TYLCAZAK, J.H. 1992. Abrasive wear. *Friction, Lubrication, and Wear Technology*. ASM Handbook, vol. 18. Materials Park, OH. pp. 184-190.
- VILAR, R. 1999. Laser cladding. *Journal of Laser Applications*, vol. 11, no. 64. pp. 64-81. ◆



becker
MINING SYSTEMS

Becker Mining Systems are market leaders in the design, manufacture & supply of:

- Electrical Switchgear & Transformers
- Collision Avoidance Systems
- Underground IT & Communication Networks
- Underground Electronic Automation
- Underground Support & Chairlift Systems
- Rope Attachments & Hoisting Equipment
- Heavy Duty Pump Solutions

Know-How. Performance. Reliability

Tel: +27 11 617 6300 Fax: +27 11 908 5806
E-mail: info@za.becker-mining.com www.za.becker-mining.com